THE ASTROPHYSICAL JOURNAL, 515:356–364, 1999 April 10
© 1999. The American Astronomical Society. All rights reserved. Printed in U.S.A.

THE VISUAL ORBIT OF ι PEGASI

A. F. BODEN,[1,2] C. D. KORESKO,[3] G. T. VAN BELLE,[1] M. M. COLAVITA,[1] P. J. DUMONT,[1] J. GUBLER,[4] S. R. KULKARNI,[3] B. F. LANE,[3] D. MOBLEY,[1] M. SHAO,[1] AND J. K. WALLACE[1] (THE PTI COLLABORATION), AND G. W. HENRY[5]

Received 1998 March 13; accepted 1998 November 18

ABSTRACT

We have determined the visual orbit for the spectroscopic binary ι Pegasi with interferometric visibility data obtained by the Palomar Testbed Interferometer in 1997. ι Peg is a double-lined binary system whose minimum masses and spectral typing suggests the possibility of eclipses. Our orbital and component diameter determinations do not favor the eclipse hypothesis: the limb-to-limb separation of the two components is 0.151 ± 0.069 mas at conjunction. Our conclusion that the ι Peg system does not eclipse is supported by high-precision photometric observations. The physical parameters implied by our visual orbit and the spectroscopic orbit of Fekel & Tomkin are in good agreement with those inferred by other means. In particular, the orbital parallax of the system is determined to be 86.9 ± 1.0 mas, and masses of the two components are determined to be 1.326 ± 0.016 and $0.819 \pm 0.009\ M_{\odot}$, respectively.

Subject headings: binaries: spectroscopic — stars: fundamental parameters — stars: individual (ι Pegasi) — techniques: interferometric

1. INTRODUCTION

ι Pegasi (HR 8430, HD 210027) is a nearby, short-period (10.2 day) binary system with a F5 V primary and a ~G8 V secondary in a circular orbit. ι Peg was first discovered as a single-line spectroscopic binary by Campbell (1899), and the first spectroscopic orbital elements were estimated by Curtis (1904). Several other single-line studies were made, notably Petrie & Phibbs (1949) and Abt & Levy (1976). In the context of a lithium abundance study, Herbig (1965) noted that lines from the ι Peg secondary were visible at red wavelengths. Lithium abundances for both the primary (Herbig 1965; Conti & Danzinger 1966; Duncan 1981; Lyubimkov, Polosukhina, & Rosgopchin 1991) and the secondary (Fekel & Tomkin 1983; Lyubimkov et al. 1991), indicate the system is very young ($\sim 8 \times 10^7$ yr, Fekel & Tomkin 1983; $1.7 \pm 0.8 \times 10^8$ yr, Lyubimkov et al. 1991) and both components are close to the zero-age main sequence. Both components of ι Peg are also believed to have solar-type abundances (Lyubimkov et al. 1991).

Following Herbig's implicit suggestion, Fekel & Tomkin (1983, hereafter FT) made radial velocity measurements of both ι Peg components at 643 nm and computed a definitive spectroscopic orbit and inferred a probable G8 V spectral classification for the secondary. FT's orbit was noteworthy as it indicated that the minimum masses for the two components were very near the model values for the spectral types, suggesting a "reasonable prospect" for eclipses in the system (FT). Subsequent photometric monitoring by automated photometry projects in Arizona, at Palomar Observatory, and in Pasadena failed to show any evidence for eclipses (see § 5). FT also questioned the synchronous rotation of the secondary. However, Gray (1984), from somewhat higher resolution spectroscopic data, argued that both components are in synchronous rotation.

Herein we report a determination of the ι Peg visual orbit from near-IR, long-baseline interferometric visibility measurements taken with the Palomar Testbed Interferometer (PTI). PTI is a 110 m K-band (2–2.4 μm) interferometer located at Palomar Observatory and described in detail elsewhere (Colavita et al. 1994, 1999). The minimum PTI fringe spacing is roughly 4 mas at the sky position of ι Peg, allowing us to resolve this binary system. The procedures we have used to determine ι Peg's visual orbit are similar to other visual orbits determined for spectroscopic binaries using the Mark III Interferometer at Mount Wilson (Pan et al. 1990, 1992; Pan, Shao, & Colavita 1993; Armstrong et al. 1992a, 1992b; Hummel et al. 1993, 1994, 1995) and the Navy Prototype Optical Interferometer at Anderson Mesa, AZ (Hummel et al. 1998). The analogy between ι Peg and the short-period, small–angular scale binaries studied in Hummel et al. (1995, 1998) is especially apt.

2. OBSERVATIONS

Pan attempted to determine a visual orbit for ι Peg using the Mark III interferometer at Mount Wilson, but the significant brightness difference in the two components at 800 nm made the observations difficult (X. Pan 1997, private communication). The apparent contrast ratio in the ι Peg system decreases in the K band, allowing a reliable orbit determination with PTI observations.

The observable used for these observations is the fringe contrast or *visibility* (squared) of an observed brightness distribution on the sky. Normalized in the interval [0, 1], a single star exhibits visibility modulus given in a uniform disk model by

$$V = \frac{2J_1(\pi B\theta/\lambda)}{\pi B\theta/\lambda}, \tag{1}$$

where J_1 is the first-order Bessel function, B is the projected baseline vector magnitude at the star position, θ is the apparent angular diameter of the star, and λ is the center-band wavelength of the interferometric observation. (We consider corrections to the uniform disk model from limb darkening in § 4.) The expected squared visibility in a

[1] Jet Propulsion Laboratory, California Institute of Technology, 4800 Oak Grove Drive, Pasadena, CA 91109.
[2] Email: bode@huey.jpl.nasa.gov.
[3] Palomar Observatory, California Institute of Technology.
[4] University of California, San Diego.
[5] Center of Excellence in Information Systems, Tennessee State University.

narrow passband for a binary star such as ι Peg is given by

$$V^2_{\rm nb}(\lambda) = \frac{V_1^2 + V_2^2 r^2 + 2V_1 V_2 r \cos\left[(2\pi/\lambda)\boldsymbol{B}\cdot\boldsymbol{s}\right]}{(1+r)^2}, \quad (2)$$

where V_1 and V_2 are the visibility moduli for the two stars alone as given by equation (1), r is the apparent brightness ratio between the primary and companion, $\boldsymbol{B}$ is the projected baseline vector at the system sky position, and $\boldsymbol{s}$ is the primary-secondary angular separation vector on the plane of the sky (Pan et al. 1990; Hummel et al. 1995). The V^2 observables used in our ι Peg study are both narrowband V^2 from seven individual spectral channels (Colavita et al. 1999) and a synthetic wide-band V^2, given by an incoherent signal-to-noise ratio–weighted average V^2 of the narrowband channels in the PTI spectrometer (Colavita 1999). In this model the expected wide-band V^2 observable is approximately given by an average of the narrowband formula over the finite passband of the spectrometer:

$$V^2_{\rm wb} = \frac{1}{n}\sum_i^n V^2_{{\rm nb}-i}(\lambda_i), \quad (3)$$

where the sum runs over the $n = 7$ channels with wavelengths λ_i covering the K band (2–2.4 μm) of the PTI spectrometer in its 1997 configuration. Separate calibrations and hypothesis fits to the narrowband and synthetic wide-band V^2 data sets yield statistically consistent results, with the synthetic wide-band data exhibiting superior fit performance. Consequently, we will present only the results from the synthetic wide-band data.

ι Peg was observed by PTI on 24 nights between 1997 July 2 and September 8. In each night ι Peg was observed in conjunction with calibration objects multiple times during the night. Each observation ("scan") was from 120–130 s in duration. For each scan we computed a mean V^2 value through methods described in Colavita (1999). We assumed the measured rms in the internal scatter to be the error in V^2. For the purposes of this analysis we have restricted our attention to four calibration objects, two primary calibrators within 5° of ι Peg (HD 211006 and HD 211432) and two ancillary calibrators within 15° of ι Peg (HD 215510 and HD 217014 − 51 Peg). The suitability of 51 Peg (a known radial-velocity variable) as a calibrator at PTI is addressed in Boden et al. (1998b). Table 1 summarizes the relevant parameters on the calibration objects used in this study. In particular, we have estimated our calibrator diameters based on a model diameter on 51 Peg of 0.72 ± 0.06 mas implied by a linear diameter of $1.2 \pm 0.1\ R_\odot$ (adopted by Marcy et al. 1997) and a parallax of 65.1 ± 0.76 mas from *Hipparcos* (ESA 1997; Perryman et al. 1997).

The calibration of ι Peg V^2 data is performed by estimating the interferometer system visibility ($V^2_{\rm sys}$) using calibration sources with model angular diameters, then normalizing the raw ι Peg visibility by $V^2_{\rm sys}$ to estimate the V^2 measured by an ideal interferometer at that epoch (Mozurkewich et al. 1991; Boden et al. 1998a). We calibrated the ι Peg V^2 data in two different ways: (1) with respect to the two primary calibration objects, resulting in our primary data set containing 112 calibrated observations over 17 nights and (2) an unbiased average of the primary and ancillary calibrators, resulting in our secondary data set containing 151 observations over 24 nights. The motivation for constructing these two data sets, which are clearly not independent, is that the determination of the orbital solution and component diameters is sensitive to calibration uncertainties. Comparison of the solutions derived from the two data sets allows us to quantitatively assess this uncertainty.

3. ORBIT DETERMINATION

The estimation of the ι Peg visual orbit is made by fitting a Keplerian orbit model with visibilities predicted by equations (2) and (3) directly to the calibrated (narrowband and synthetic wide-band) V^2 data on ι Peg (see Armstrong et al. 1992b; Hummel et al. 1993, 1995). The fit is nonlinear in the Keplerian orbital elements and is therefore performed by nonlinear least-squares methods (i.e., the Marquardt-Levenberg method; Press et al. 1992). As such, this fitting procedure takes an initial estimate of the orbital elements and other parameters (e.g., component angular diameters, brightness ratio) and refines the model into a new parameter set that best fits the data. However, the χ^2 surface has many local minima in addition to the global minimum corresponding to the true orbit. Because Marquardt-Levenberg strictly follows a downhill path in the χ^2 manifold, it is necessary to thoroughly survey the space of possible binary parameters in order to distinguish between local minima and the true global minimum. In the case of ι Peg the parameter space is significantly narrowed by the high-quality spectroscopic orbit and inclination constraint near 90° (FT). Furthermore, the *Hipparcos* distance determination sets the rough scale of the semimajor axis (ESA 1997).

In addition, as the V^2 observable for the binary (eqs. [2] and [3]) is invariant under a rotation of 180°, we cannot differentiate between an apparent primary/secondary relative orientation and its mirror image on the sky. In order to follow the FT convention for T_0 at primary radial velocity maximum, in our analysis of ι Peg we have defined T_0 to be at a component separation extremum, yielding an extre-

TABLE 1

1997 PTI ι PEG CALIBRATION OBJECTS CONSIDERED IN OUR ANALYSIS

Object Name	Spectral Type	Star Magnitude (V/K)	Sky Separation from ι Peg (deg)	Diameter of WRT Model 51 Peg
HD 211006.....	K2III	5.9/3.4	3.6	1.06 ± 0.05
HD 211432.....	G9III	6.4/3.7	3.2	0.70 ± 0.05
HD 215510.....	G6III	6.3/3.9	11	0.85 ± 0.06
HD 217014.....	G2.5 V	5.9/4.0	12	(0.72 ± 0.06)

NOTE.—The relevant parameters for our four calibration objects are summarized. The apparent diameter values are determined by a fit to our V^2 data calibrated with respect to a model diameter for HD 217014 (51 Peg) of 0.72 ± 0.06 mas (Marcy et al. 1997; ESA 1997).

mum in component radial velocities for the circular orbit. We have additionally required our fit T_0 to be within half a period of the projected FT determination in order to differentiate between primary radial velocity maximum and minimum. Even with our determination of T_0 so defined, there remains a 180° ambiguity in our determination of the longitude of the ascending node, Ω.

We used a preliminary orbital solution computed by Pan et al. (1996) by separation vector techniques (see Pan et al. 1990 for a discussion of the method) and refined it into the best-fit orbit shown here. We further conducted an exhaustive search of the binary parameter space that resulted in the same best-fit orbit, which is in fact the global minimum in the χ^2 manifold.

Figure 1 depicts the apparent relative orbit of the ι Peg system. Most striking is the observation that the circular orbit of the system (see below) is very nearly eclipsing. From our primary data set we find a best-fit orbital inclination of 95.67° ± 0.21°. With model angular diameters of 1.0 and 0.7 mas for the primary and secondary components, respectively (§ 4), and an apparent semimajor axis of 10.33 ± 0.10 mas, this inclination is about 0°.87 from apparent limb-to-limb contact. This is consistent with the lack of photometric evidence for eclipses despite several photometry campaigns on the ι Peg system (§ 5).

Table 2 lists the complete set of V^2 measurements in the primary data set and the prediction based on the best-fit orbit model for ι Peg. Figure 2 shows two graphical comparisons between our V^2 data on ι Peg and the best-fit model predictions. Figure 2*a* gives four consecutive nights of PTI V^2 data from our primary data set on ι Peg (1997 July 18–21) and V^2 predictions based on the best-fit model for the system. Figure 2*b* gives an additional seven consecutive nights (1997 August 12–18) with the same quantities plotted. These are the two longest consecutive-night sequences in our data set. The model predictions are seen to be in excellent absolute and statistical agreement with the observed data, with a primary data set average, absolute V^2 deviation of 0.014 and a χ^2 per degree of freedom (DOF) of 0.75.

Figure 3 gives two examples of the χ^2 fit projected into orbital parameter subspaces. Figure 3*a* shows a surface of

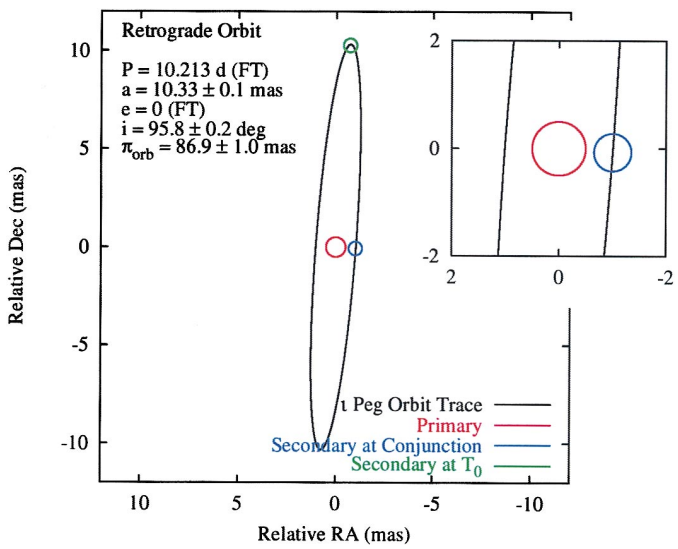

FIG. 1.—Visual orbit of ι Peg. The relative visual orbit of ι Peg is depicted, with the primary and secondary rendered at T_0 (maximum primary radial velocity) and apparent conjunction. The inset shows a closeup of the system at apparent conjunction. By our model the ι Peg orbit is nearly but not quite eclipsing, being approximately 0°.87 in inclination from apparent grazing eclipses.

χ^2/DOF projected into the subspace of orbit semimajor axis and relative component brightness, with all other parameters held to their best-fit values. Inset is a closeup of a contour plot of the χ^2/DOF surface indicating location of the best-fit parameter values and contours at +1, +2, and +3 of χ^2/DOF significance. Figure 3*b* gives the χ^2/DOF surface in the subspace of orbital inclination and longitude of the ascending node. Again, the inset gives best-fit parameter values and contours at +1, +2, and +3 of χ^2/DOF significance. All indications are that the best-fit model for the ι Peg system is in excellent agreement with our V^2 data and that data uniquely constrain the parameters of the visual orbit.

Spectroscopic (from FT) and visual orbital parameters of the ι Peg system are summarized in Table 3. We present the results for our primary and secondary data sets separately. For the parameters we have estimated from our interfero-

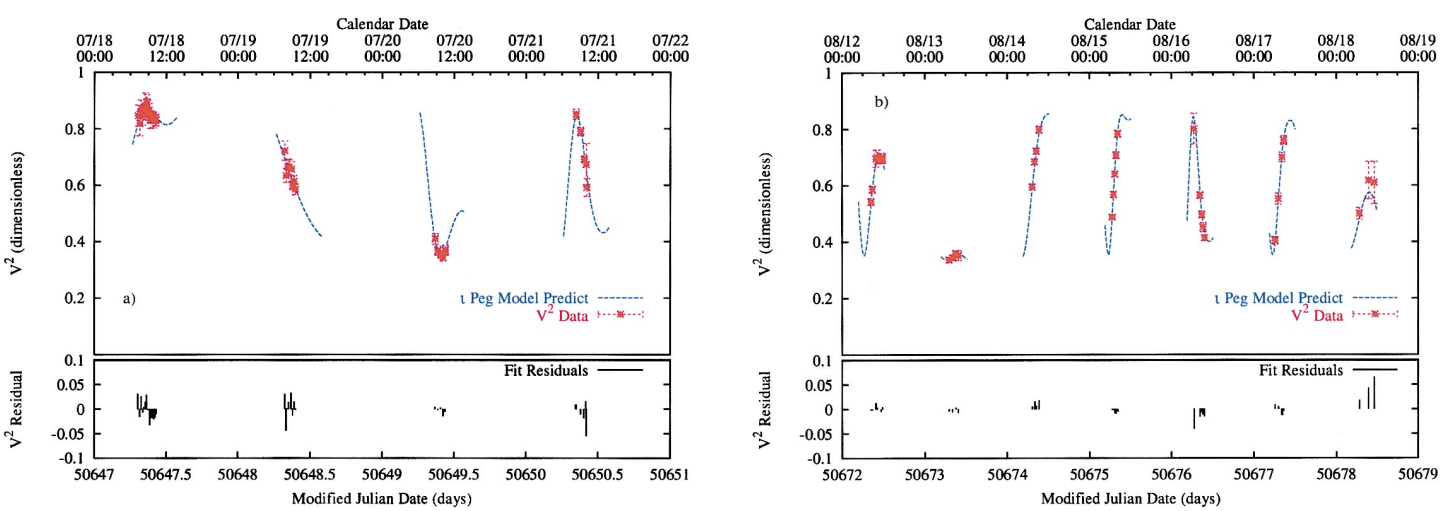

FIG. 2.—V^2 fit of ι Peg. (*a*) Four consecutive nights (1997 July 18–21) of calibrated V^2 data on ι Peg and V^2 predictions from the best-fit model for the system. In the lower frame we give V^2 residuals between the calibrated data and the best-fit model. (*b*) An additional seven consecutive nights (1997 August 12–18) of data on ι Peg, with model predicts and fit residuals. The model is in good agreement with the calibrated data, with a χ^2/DOF of 0.75 and an average absolute V^2 residual of 0.014.

TABLE 2

ι Peg Primary Data Set, Best-Fit Model Predictions, and Residuals

Julian Date	Calendar Date	UT	Measured V^2	Error	V^2 Model Prediction	V^2 Residual
50647.80181.....	1997 Jul 18	7:14:36	0.846	0.038	0.815	0.031
50647.81556.....		7:34:23	0.819	0.043	0.835	−0.016
50647.82495.....		7:47:55	0.872	0.030	0.846	0.026
50647.83541.....		8:02:59	0.849	0.036	0.855	−0.007
50647.84728.....		8:20:04	0.866	0.022	0.862	0.004
50647.85482.....		8:30:56	0.880	0.047	0.865	0.015
50647.86287.....		8:42:31	0.895	0.026	0.866	0.029
50647.87229.....		8:56:06	0.865	0.036	0.866	−0.001
50647.87981.....		9:06:55	0.865	0.024	0.865	0.000
50647.88748.....		9:17:58	0.830	0.030	0.863	−0.032
50647.89693.....		9:31:34	0.841	0.021	0.859	−0.018
50647.90395.....		9:41:41	0.841	0.015	0.855	−0.014
50647.9113		9:52:15	0.830	0.028	0.851	−0.021
50647.92058.....		10:05:38	0.828	0.019	0.846	−0.018
50647.92789.....		10:16:09	0.832	0.020	0.841	−0.009
50648.82444.....	1997 Jul 19	7:47:11	0.722	0.035	0.691	0.031
50648.83364.....		8:00:26	0.634	0.025	0.677	−0.043
50648.84342.....		8:14:31	0.664	0.028	0.663	0.001
50648.85301.....		8:28:20	0.662	0.028	0.648	0.014
50648.86952.....		8:52:06	0.657	0.026	0.624	0.032
50648.87877.....		9:05:25	0.599	0.016	0.612	−0.013
50648.88843.....		9:19:20	0.613	0.021	0.598	0.015
50648.89773.....		9:32:43	0.585	0.019	0.586	−0.000
50649.86696.....	1997 Jul 20	8:48:25	0.409	0.019	0.405	0.004
50649.88384.....		9:12:43	0.368	0.015	0.369	−0.002
50649.90416.....		9:41:59	0.356	0.014	0.353	0.003
50649.9217		10:07:14	0.344	0.013	0.359	−0.015
50649.93655.....		10:28:37	0.369	0.017	0.375	−0.006
50650.84729.....	1997 Jul 21	8:20:05	0.851	0.018	0.842	0.009
50650.87801.....		9:04:19	0.790	0.015	0.800	−0.010
50650.90195.....		9:38:48	0.691	0.012	0.710	−0.019
50650.91566.....		9:58:32	0.673	0.075	0.657	0.016
50650.91948.....		10:04:02	0.592	0.031	0.646	−0.055
50659.83293.....	1997 Jul 30	7:59:25	0.774	0.018	0.775	−0.001
50659.84011.....		8:09:45	0.805	0.022	0.753	0.052
50659.86826.....		8:50:17	0.656	0.024	0.657	−0.001
50659.87567.....		9:00:57	0.649	0.017	0.632	0.017
50659.90534.....		9:43:41	0.554	0.017	0.543	0.011
50659.91225.....		9:53:38	0.549	0.017	0.525	0.024
50659.94485.....		10:40:35	0.479	0.018	0.457	0.022
50659.95221.....		10:51:10	0.453	0.015	0.445	0.008
50659.98217.....		11:34:19	0.434	0.024	0.411	0.023
50659.98931.....		11:44:36	0.427	0.025	0.407	0.020
50660.81914.....	1997 Jul 31	7:39:33	0.786	0.022	0.783	0.003
50660.8346		8:01:49	0.850	0.018	0.829	0.021
50660.85318.....		8:28:34	0.839	0.029	0.845	−0.006
50660.86865.....		8:50:51	0.857	0.028	0.831	0.026
50660.89155.....		9:23:49	0.779	0.033	0.775	0.004
50660.90886.....		9:48:45	0.716	0.028	0.722	−0.006
50660.93543.....		10:27:01	0.619	0.039	0.643	−0.023
50660.95022.....		10:48:18	0.606	0.019	0.609	−0.003
50660.96569.....		11:10:35	0.612	0.031	0.585	0.027
50660.98055.....		11:31:59	0.577	0.022	0.565	0.011
50660.99702.....		11:55:42	0.533	0.048	0.555	−0.021
50661.00991.....		12:14:16	0.474	0.033	0.549	−0.075
50661.81235.....	1997 Aug 01	7:29:47	0.871	0.027	0.837	0.033
50661.82807.....		7:52:25	0.850	0.030	0.842	0.008
50661.84898.....		8:22:31	0.830	0.026	0.805	0.024
50661.86423.....		8:44:29	0.784	0.019	0.756	0.028
50661.8849		9:14:15	0.694	0.014	0.678	0.016
50661.89919.....		9:34:50	0.638	0.015	0.626	0.012
50661.9217		10:07:15	0.570	0.013	0.558	0.012
50661.93594.....		10:27:44	0.538	0.011	0.526	0.012
50661.9566		10:57:30	0.498	0.014	0.495	0.003
50661.97175.....		11:19:19	0.478	0.022	0.481	−0.003
50661.998		11:57:07	0.472	0.018	0.473	−0.002

TABLE 2—*Continued*

Julian Date	Calendar Date	UT	Measured V^2	Error	V^2 Model Prediction	V^2 Residual
50672.84939.....	1997 Aug 12	8:23:07	0.542	0.012	0.544	−0.002
50672.86492.....		8:45:28	0.586	0.012	0.588	−0.001
50672.91048.....		9:51:05	0.695	0.030	0.682	0.013
50672.92547.....		10:12:40	0.702	0.025	0.699	0.003
50672.97332.....		11:21:35	0.699	0.017	0.704	−0.005
50672.98845.....		11:43:22	0.696	0.018	0.692	0.004
50673.79096.....	1997 Aug 13	6:58:59	0.336	0.010	0.340	−0.004
50673.83522.....		8:02:42	0.344	0.010	0.349	−0.006
50673.87336.....		8:57:37	0.360	0.007	0.357	0.003
50673.90543.....		9:43:49	0.352	0.017	0.358	−0.007
50674.80151.....	1997 Aug 14	7:14:10	0.594	0.011	0.589	0.005
50674.83068.....		7:56:10	0.684	0.009	0.668	0.016
50674.84999.....		8:23:58	0.722	0.010	0.714	0.007
50674.88467.....		9:13:55	0.798	0.013	0.780	0.018
50675.77741.....	1997 Aug 15	6:39:28	0.488	0.007	0.488	−0.001
50675.79329.....		7:02:20	0.567	0.011	0.569	−0.002
50675.80871.....		7:24:32	0.640	0.011	0.648	−0.008
50675.82331.....		7:45:34	0.706	0.012	0.715	−0.008
50675.84494.....		8:16:42	0.782	0.013	0.788	−0.005
50676.77174.....	1997 Aug 16	6:31:18	0.801	0.054	0.841	−0.040
50676.8422		8:12:45	0.565	0.011	0.580	−0.016
50676.86442.....		8:44:45	0.496	0.012	0.502	−0.006
50676.87941.....		9:06:21	0.452	0.016	0.462	−0.011
50676.89791.....		9:32:59	0.413	0.010	0.428	−0.014
50677.7532	1997 Aug 17	6:04:36	0.404	0.013	0.395	0.009
50677.79427.....		7:03:45	0.552	0.020	0.546	0.006
50677.83911.....		8:08:19	0.700	0.018	0.713	−0.013
50677.85929.....		8:37:22	0.760	0.015	0.764	−0.004
50678.7794	1997 Aug 18	6:42:19	0.500	0.021	0.482	0.018
50678.89388.....		9:27:10	0.617	0.066	0.575	0.042
50678.96302.....		11:06:44	0.609	0.075	0.545	0.065
50681.78315.....		6:47:44	0.792	0.023	0.787	0.005
50681.82948.....	1997 Aug 21	7:54:27	0.593	0.014	0.587	0.006
50681.85704.....		8:34:07	0.483	0.013	0.491	−0.007
50684.7004	1997 Aug 24	4:48:34	0.437	0.022	0.452	−0.015
50684.71621.....		5:11:20	0.444	0.019	0.423	0.021
50684.73825.....		5:43:04	0.395	0.020	0.390	0.005
50684.77121.....		6:30:32	0.329	0.012	0.356	−0.027
50684.81539.....		7:34:09	0.346	0.011	0.338	0.009
50684.83993.....		8:09:30	0.335	0.009	0.339	−0.004
50684.85529.....		8:31:36	0.341	0.007	0.343	−0.002
50684.89971.....		9:35:34	0.363	0.010	0.361	0.002
50684.93043.....		10:19:49	0.381	0.014	0.375	0.005
50699.80539.....	1997 Sep 08	7:19:45	0.890	0.023	0.879	0.011
50699.85183.....		8:26:37	0.843	0.020	0.878	−0.035
50699.88659.....		9:16:41	0.887	0.023	0.871	0.016

metric data, we quote a total 1 σ error in the parameter estimates and the 1 σ errors in the parameter estimates from statistical (measurement uncertainty) and systematic error sources. In our analysis the dominant forms of systematic error are (1) uncertainties in the calibrator angular diameters (Table 1); (2) the uncertainty in our center-band operating wavelength ($\lambda_0 \approx 2.2$ μm), which we have taken to be 20 nm ($\sim 1\%$); (3) the geometrical uncertainty in our interferometric baseline (less than 0.01%); and (4) uncertainties in orbital parameters we have constrained in our fitting procedure (e.g., period, eccentricity). Different parameters are affected differently by these error sources; our estimated uncertainty in the ι Peg orbital inclination is dominated by measurement uncertainty, while the uncertainty in the angular semimajor axis is dominated by uncertainty in the wavelength scale. Conversely, we have assumed that all the uncertainty quoted by FT in the ι Peg spectroscopic parameters is statistical. Finally, we have listed the level of statistical agreement in the visual orbit parameters in our two solutions (the absolute residual between the two estimates divided by the RSS of their statistical errors). The two solutions are in good statistical agreement, giving us confidence we have properly characterized our calibration uncertainties.

Particularly remarkable is the agreement between T_0 (quoted as the epoch of maximum primary radial velocity for the ι Peg circular orbit) and period as determined by FT and T_0 as determined in our primary data set, separated from the FT determination by 523 cycles. FT quotes an ι Peg period accurate to roughly 1 part in 10^6, resulting in a propagated uncertainty in T_0 at the epoch of our observations of 7×10^{-3} days. This FT-extrapolated T_0 differs from our 1997 T_0 determination by 8×10^{-4} days, which is an agreement of roughly 0.1 σ. A similar comparison with

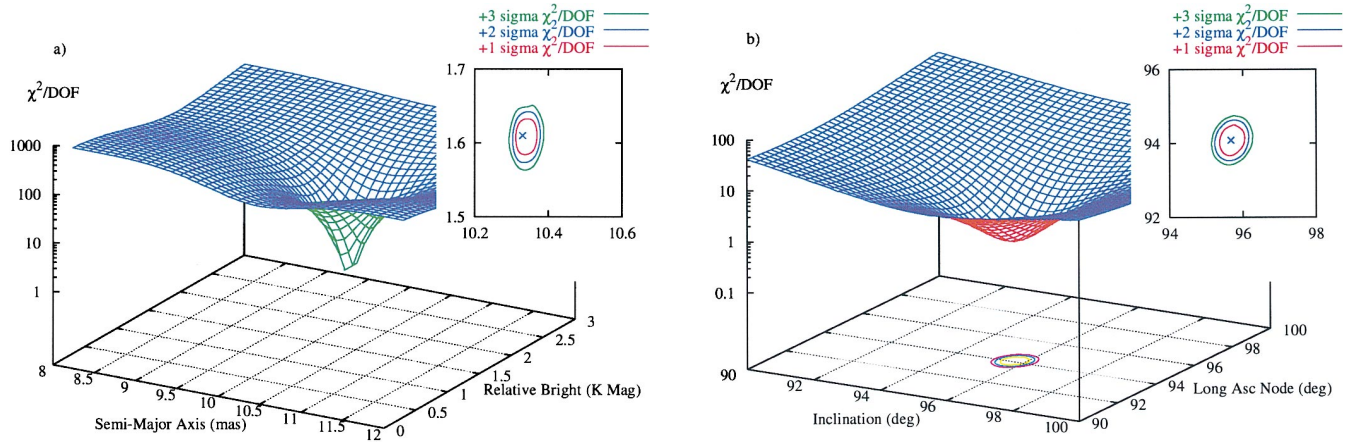

FIG. 3.—χ^2/DOF fit surfaces for ι Peg primary data set. (*a*) χ^2/DOF surface in the subspace of orbit semimajor axis and relative component brightness. The inset is a closeup of a contour plot surface indicating location of the best-fit parameter values and contours at +1, +2, and +3 of χ^2/DOF significance. (*b*) χ^2/DOF surface in the subspace of orbital inclination and longitude of the ascending node, with the inset giving surface contour closeup.

the secondary data set solution is less spectacular, an agreement at 0.7 σ. Clearly the extraordinary quoted accuracy of the ι Peg period determination by FT (made by combining their 1977–1982 data with spectroscopy from the mid-30s; Petrie & Phibbs 1949) seems well justified compared with our visual orbit. Consequently, we have assumed the FT value for the ι Peg period.

Following FT, we have assumed a circular orbit for the system. Fitting our primary data set for an eccentricity in the system yields an estimate of $1.5 \times 10^{-3} \pm 1.3 \times 10^{-3}$. The assumption of a circular orbit seems well justified.

4. PHYSICAL PARAMETERS

Physical parameters derived from the ι Peg primary data set visual orbit and the FT spectroscopic orbit are summarized in Table 4. We use the primary data set solution because it is the most free from possible sky position–dependent systematic effects (as the secondary data set includes the ancillary calibrators), but we note that the two orbital solutions yield statistically consistent results. Notable among the physical parameters for the system is the high-precision determination of the component masses for the system, a virtue of the precision of the FT radial velocities on both components and the high inclination of the orbit. We estimate the masses of the F5 V primary and putative G8 V secondary components as 1.326 ± 0.016 and $0.819 \pm 0.009\ M_\odot$, respectively. Our mass values agree well with mass estimates of 1.33 ± 0.08 and $0.9 \pm 0.2\ M_\odot$,

TABLE 3

ORBITAL PARAMETERS FOR ι PEG

		PTI 1997		
ORBITAL PARAMETER	FT 1983	Primary Data Set	Secondary Data Set	Statistical Agreement
Period (d)	10.213033 $\pm 1.3 \times 10^{-5}$	10.213033 (assumed)	10.213033 (assumed)	
T_0 (HJD)	2445320.1423	2450661.5578 ± 3.6 (3.3/1.5) $\times 10^{-3}$	2450661.5634 ± 3.3 (3.0/1.5) $\times 10^{-3}$	1.26
e	0 (assumed)	0 (assumed)	0 (assumed)	
K_A (km s^{-1})	48.1 ± 0.2			
K_B (km s^{-1})	77.9 ± 0.3			
i (deg).....		95.67 ± 0.22 (0.22/0.03)	96.03 ± 0.20 (0.20/0.03)	1.21
Ω (deg)		94.09 ± 0.23 (0.22/0.05)	94.03 ± 0.25 (0.24/0.05)	0.03
a (mas)		10.33 ± 0.10 (0.02/0.10)	10.32 ± 0.11 (0.02/0.11)	0.35
Δ K (mag)		1.610 ± 0.021 (0.007/0.020)	1.610 ± 0.021 (0.007/0.020)	0.23
χ^2/DOF		0.75	1.0	
$\overline{\lvert R_{V^2} \rvert}$		0.014	0.016	
$N_{\rm scans}$		112	151	

NOTE.—Summarized here are the apparent orbital parameters for the ι Peg system as determined by FT and our PTI primary and secondary data sets. For parameters estimated from our PTI observations, we separately quote 1 σ errors from both statistical and systematic sources (listed as $\sigma_{\rm stat}/\sigma_{\rm sys}$) and the total error as the sum of the two in quadrature. We have also included the level of statistical agreement between visual orbit parameters from our two solutions; the parameters estimated separately from the primary and secondary data sets are in good agreement in relation to the statistical component of their error estimates. We have quoted the longitude of the ascending node parameter (Ω) as the angle between local east and the orbital line of nodes (and the relative position of the secondary at T_0), measured positive in the direction of local north. Because of the degeneracy in our V^2 observable, there is a 180° ambiguity in Ω. Finally, the fit χ^2/DOF and mean absolute V^2 residual ($\overline{\lvert R_{V^2} \rvert}$) is listed for both solutions.

TABLE 4

PHYSICAL PARAMETERS FOR ι PEG

Physical Parameter	Primary Component	Secondary Component
a (10^{-2} AU)	4.54 ± 0.03 (0.03/0.0002)	7.35 ± 0.03 (0.03/0.0003)
Mass ($M_\odot$)	1.326 ± 0.016 (0.016/0.0001)	0.819 ± 0.009 (0.009/0.0001)
Sp Type (FT)	F5V	G8V
Model Diameter (mas)	1.0	0.7
UD Fit Diameter (mas)	0.98 ± 0.05 (0.01/0.05)	0.70 ± 0.10 (0.03/0.10)
LD Fit Diameter (mas)	1.0 ± 0.05 (0.01/0.05)	0.71 ± 0.10 (0.03/0.10)
System Distance (pc)	11.51 ± 0.13 (0.05/0.12)	
π_{orb} (mas)	86.91 ± 1.0 (0.34/0.94)	
M_K (mag)	2.574 ± 0.025 (0.010/0.024)	4.182 ± 0.030 (0.019/0.028)

NOTE.—Summarized here are the physical parameters for the ι Peg system as derived from the orbital parameters in Table 3. As for our PTI-derived orbital parameters, we have quoted both total error and separate contributions from statistical and systematic sources (given as $\sigma_{stat}/\sigma_{sys}$).

respectively, made by Lyubimkov et al. (1991) based on evolutionary models and spectroscopic measurements of component effective temperatures and surface gravities.

The *Hipparcos* catalog lists the parallax of ι Peg as 85.06 ± 0.71 mas (ESA 1997). The distance determination to ι Peg based on the FT radial velocities and our apparent semimajor axis and inclination is 11.51 ± 0.13 pc, corresponding to an orbital parallax of 86.91 ± 1.0 mas, which is consistent with the *Hipparcos* result at roughly 2% and 1.5 σ.

FT lists main-sequence model linear diameters for the two ι Peg components as 1.3 and 0.9 $R_\odot$, respectively (FT). At a distance of approximately 11.5 pc, this corresponds to apparent angular diameters of 1.0 and 0.7 mas for the primary and secondary components, respectively. We have fitted for the uniform-disk angular diameter for both components as a part of the orbit estimation and find best-fit apparent diameters of 0.98 ± 0.05 and 0.70 ± 0.10 mas. Because we have limited spatial frequency coverage in our data, following Mozurkewich et al. (1991) and Quirrenbach et al. (1996) we have estimated the limb-darkened diameters of the components from a correction to the uniform-disk diameter based on the solar limb darkening at 2 μm given by Allen (1982). The limb-darkened diameters for the primary and secondary components are 1.0 ± 0.05 and 0.71 ± 0.10 mas, respectively. For both the primary and secondary components our fits for apparent diameter are in good agreement with main-sequence model diameters.

The observed K magnitude of the ι Peg system (2.623 ± 0.016, Carrasco et al. 1991; 2.656 ± 0.002, Bouchet, Manfroid, & Schmider 1991) and our estimates of the distance and relative K photometry (Table 3) of the system allows the determination of the absolute magnitude of both components separately. Using the Bouchet et al. (1991) K photometry we obtain M_K values of 2.574 ± 0.025 and 4.182 ± 0.030 for the primary and secondary components, respectively. Both of these M_K values are consistent (within quoted scatter) with the empirical mass-luminosity relation for nearby low-mass, main-sequence stars given by Henry & McCarthy (1992, 1993). In particular, our M_K value for the primary is 0.010 mag brighter than the mass-luminosity prediction (Henry & McCarthy 1992), while the 4.18 M_K value for the secondary is roughly 0.28 mag dimmer than the prediction (Henry & McCarthy 1993). Both values are well within the quoted scatter of the mass-luminosity models. A second check on the absolute K magnitude estimates can be extracted from the model calculations of Bertelli et al. (1994), who predict absolute K magnitudes of 2.616 ± 0.048 and 4.254 ± 0.039 for our estimated primary and secondary masses, respectively, for main-sequence stars with solar-type abundances at an age of $1.7 \pm 0.8 \times 10^8$ yr (Lyubimkov et al. 1991).

5. ECLIPSE SEARCH

A critical test of our visual orbit model is a high-precision photometric search for eclipses in ι Peg. Combined with our visual orbit (Table 3), our measured diameters (Table 4) imply an apparent limb-to-limb separation at a conjunction of 0.151 ± 0.069 mas (using our limb-darkened diameter estimates). Our visual orbit and fit diameters do not favor the FT conjecture of possible eclipses in the ι Peg system. Conversely, were the inclination of the orbit near 90°, there would be significant primary eclipses with a duration of a few hours (6.8 hr for $i = 90°$; FT) and as large as 0.6 mag in the V band.

Several individuals have searched for signs of eclipses in the ι Peg system. In 1997 both D. Van Buren (1997, private communication) with the 60″ telescope at Palomar and one of us (C. D. K.) at the Robinson Rooftop Observatory at Caltech in Pasadena (Koresko 1997) searched for eclipses during primary and secondary eclipse opportunities, respectively. Both searches resulted in nondetections at about the 0.1 mag levels.

More comprehensive and sensitive than the Southern California searches has been the program conducted by the Automated Astronomy Group at Tennessee State University. ι Peg was observed photometrically in 1984 with the Phoenix-10 automatic photoelectric telescope (APT) in Phoenix, AZ and again in 1997–1998 with the Vanderbilt/Tennessee State 16 inch APT at Fairborn Observatory near Washington Camp, AZ in order to search for possible eclipses suggested by FT. Both telescopes observed ι Peg once per night through a Johnson V filter with respect to the comparison star HR 8441 (HD 210210, F1 IV) in the sequence C, V, C, V, C, V, C, where C is the comparison star and V is ι Peg. Three differential magnitudes (in the sense V-C) were computed from each nightly sequence, corrected for differential extinction, and transformed to the Johnson system. The three differential magnitudes from each sequence were then averaged together and treated as single observations thereafter. Because of the lack of accurate standardization in the Phoenix-10 data set, a -0.027 mag correction was added to each observation to bring those data in line with the 16 inch observations. The observations

TABLE 5

SUMMARY OF APT PHOTOMETRY ON ι PEG

APT	JD Range (+2400000)	Number of Observations	Standard Deviation (mag)
10 inch.....	45703–46065	78	0.0109
16 inch.....	50718–50829	66	0.0032

are summarized in Table 5. The fourth column gives the standard deviation of a single nightly observation from the mean of the entire data set and represents a measure of the precision of the observations. Further details on the telescopes, data acquisition, reductions, and quality control can be found in Young et al. (1991) and Henry (1995a, 1995b).

The photometric observations summarized in Table 5 are plotted in Figure 4 against the orbital phase of the binary computed from the FT-defined T_0 and period. For inclinations allowing eclipses of the two components, the phases of conjunction coinciding with primary and secondary eclipse opportunities are 0.25 and 0.75, respectively. FT estimated the total duration of a central eclipse ($i = 90°$) to be roughly 6.8 hr or 0.027 phase units. Our photometric observations exclude this possibility and show no evidence for any partial eclipse to a precision of around 0.003 mag. The time of conjunction is uncertain by no more than a few minutes, and gaps in the data around the time of conjunction are no larger than about 0.005 phase units (1.2 hr). Thus the possibility of all but the briefest of grazing eclipses are excluded by the APT photometry. In particular, using the two points nearest the primary conjunction opportunity (at -1.29 and $+1.22$ hr relative to the predicted conjunction, respectively) constrain $|90 - i|$ to be greater than 4°.07 and 4°.10, respectively, at greater than 99% confidence, based on the model diameters and M_v estimates of 3.4 and 5.8 for the primary and secondary components, respectively.

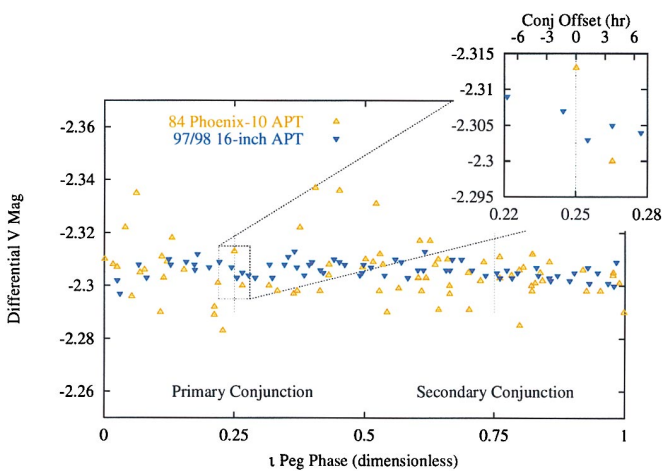

FIG. 4.—Photometric observations of ι Peg. Differential photometric observations of ι Peg from the Phoenix-10 APT (*open triangles*) and the Vanderbilt/Tennessee State University 16 inch APT (*filled triangles*) plotted against orbital phase of the binary computed following FT. Phase 0.25 represents a time of conjunction with the secondary in front (primary eclipse opportunity). In the inset we show a closeup of the data around the primary eclipse opportunity. (We have added a second horizontal scale relative to the eclipse opportunity in units of hours; a full eclipse in the ι Peg system would be roughly 7 hr in duration.) The photometric observations exclude the possibility of all but the briefest of grazing eclipses in the ι Peg system.

The components of most close binaries with orbital periods less than about 1 month rotate synchronously with the orbital period because of tidal action between the components (e.g., Fekel & Eitter 1989). Such synchronous rotation is expected in ι Peg and is confirmed by the rotational broadening measurements of FT and Gray (1984; see Wolff & Simon 1997). If the G8 V secondary, which is much more convective than the F5 V primary, is rotating synchronously, it would be expected to be photometrically variable on the orbital period at the level of a few percent because of starspot activity (Henry et al. 1999). In fact, ι Peg is listed as a suspected variable star by Petit (1990), who reports variability at the 0.02 mag level in V. FT estimate that the secondary is roughly 2.7 mag fainter in the V band than the primary, so any apparent photometric variability of the secondary component will be diluted by a factor of about 12 by the primary component.

In order to search for this possible photometric variability in ι Peg, we performed a periodogram analysis of the 16 inch APT data. The analysis reveals a photometric period that is identical within its uncertainty to the spectroscopic period, a result that is consistent with the assumption of synchronous rotation. Likewise, the amplitude of 0.0037 mag, scaled by a factor of 12, results in a 4.4% variation, which is similar to the variability expected from rotational modulation of the spotted surface of the secondary diluted by the emission of the primary. Based on these results, we conclude that ι Peg is a low-amplitude variable star.

6. SUMMARY

We have presented the visual orbit for the double-lined binary system ι Peg and derived the physical parameters of the system by combining it with the earlier spectroscopic orbit of Fekel & Tomkin. The derived physical parameters of the two young stars in ι Peg are in reasonable agreement with the results of other studies of the system and theoretical expectations for stars of these types. As was noted by FT, the ι Peg system is nearly eclipsing; because our model visual orbit is so close to producing observable eclipses, we have further presented high-precision photometric data that is consistent with our visual orbit model.

ι Peg represents a prototype of the binary system that PTI is well suited to measure; the large magnitude difference between components in the visible is significantly mitigated in the near-IR, making the accurate determination of the system parameters feasible.

Part of the work described in this paper was performed at the Jet Propulsion Laboratory, California Institute of Technology under contract with NASA. Interferometer data was obtained at the Palomar Observatory using the NASA Palomar Testbed Interferometer, which is supported by NASA contracts to the Jet Propulsion Laboratory.

Automated astronomy at TSU has been supported for several years by NASA and by the National Science Foun-

dation, most recently through NASA grants NCC2-977 and NCC5-228 (which supports TSU's Center for Automated Space Science) and NSF grants HRD-9550561 and HRD-9706268 (which supports TSU's Center for Systems Science Research).

We wish to thank the anonymous referee for his many positive contributions to the accuracy and quality of this manuscript and his forbearance in the review process.

This research has made use of the SIMBAD database, operated at CDS, Strasbourg, France.

REFERENCES

Abt, H., & Levy, S. 1976, ApJS, 30, 273
Allen, C. W. 1982, Astrophysical Quantities (London: Athlone Press)
Armstrong, J. T., et al. 1992a, AJ, 104, 241
———. 1992b, AJ, 104, 2217
Bertelli, G., Bressan, A., Chiosi, C., Fagotto, F., & Nasi, E. 1994, A&AS, 106, 275
Boden, A. F., et al. 1998a, Proc. SPIE, 3350, 872
———. 1998b, ApJ, 504, L39
Bouchet, P., Manfroid, J., & Schmider, F. X. 1991, A&AS, 91, 409
Campbell, W. W. 1899, ApJ, 9, 310
Carrasco, L., Recillas-Cruz, E., Garcia-Barreto, A., Cruz-Gonzalez, I., & Serrano, A. 1991, PASP, 103, 987
Colavita, M. 1999, PASP, in press
Colavita, M. M., et al. 1994, Proc. SPIE, 2200, 89
———. 1999, ApJ, 510, 505
Conti, P. S., & Danziger, I. J. 1966, ApJ, 146, 383
Curtis, H. D. 1904, Lick Obs. Bull., 2, 172
Duncan, D. K. 1981, ApJ, 248, 651
ESA. 1997, ESA SP-1200, The *Hipparcos* and Tycho Catalogues (Paris: ESA)
Fekel, F. C., & Eitter, J. J. 1989, AJ, 97, 1139
Fekel, F., & Tomkin, J. 1983, PASP, 95, 1000 (FT)
Gray, D. F. 1984, PASP, 96, 537
Henry, G. W. 1995a, in ASP Conf. Ser. 79, Robotic Telescopes: Current Capabilities, Present Developments, and Future Prospects for Automated Astronomy, ed. G. W. Henry & J. A. Eaton (San Francisco: ASP), 37
———. 1995b, in ASP Conf. Ser. 79, Robotic Telescopes: Current Capabilities, Present Developments, and Future Prospects for Automated Astronomy, ed. G. W. Henry & J. A. Eaton (San Francisco: ASP), 44
Henry, G. W., et al. 1999, in preparation
Henry, T., & McCarthy, D. 1992, in ASP Conf. Ser. 32, IAU Colloq. 135, Complementary Approaches to Double and Multiple Star Research, ed. H. McAllister & W. Hartikopf (San Francisco: ASP), 10
———. 1993, AJ, 106, 773
Herbig, G. H. 1965, ApJ, 141, 588
Hummel, C. A., et al. 1993, AJ, 106, 2486
———. 1994, AJ, 107, 1859
———. 1995, AJ, 110, 376
———. 1998, AJ, 116, 2536
Koresko, C. D. 1997, http://gulliver.gps.caltech.edu/PTI/iota_Peg/iota_Peg_lightcurve.html
Lyubimkov, L. S., Polosukhina, N. S., & Rosgopchin, S. I. 1991, Astrofizika, 34, 149
Marcy, G. W., Butler, R. P., Williams, E., Bildsten, L., Graham, J. R., Ghez, A. M., & Jernigan, J. G. 1997, ApJ, 481, 926
Mozurkewich, D., et al. 1991, AJ, 101, 2207
Pan, X., et al. 1990, ApJ, 356, 641
———. 1996, BAAS, 189, 32.03
Pan, X., Shao, M., & Colavita, M. 1993, ApJ, 413, L129
Pan, X., Shao, M., Colavita, M. M., Mozurkewich, D., Simon, R. S., & Johnston, K. J. 1992, ApJ, 384, 624
Perryman, M. A. C., et al. 1997, A&A, 323, L49
Petit, M. 1990, A&AS, 85, 971
Petrie, R. M., & Phibbs, E. 1949, Publ. Dom. Astrophys. Obs. Victoria, 7, 205
Press, W. H., Teukolsky, S. A., Vetterling, W. T., & Flannery, B. P. 1992, Numerical Recipes in C: The Art of Scientific Computing, 2nd Ed. (Cambridge: Cambridge Univ.)
Quirrenbach, A., et al. 1996, A&A, 312, 160
Wolff, S. C., & Simon, T. 1997, PASP, 109, 759
Young, A. T., et al. 1991, PASP, 103, 221